GLL

Geomatics, Landmanagement and Landscape No. 3 • 2024, 87–100

ISSN 2300-1496 http://dx.doi.org/10.15576/GLL/2024.3.06

Research paper

Received: 6.08.2024
Accepted: 15.08.2024
Published: 26.09.2024

Impact of image file formats on the accuracy of photogrammetric models: A comparative analysis

Hubert Aleksander Małyszek[1], ✉
Bartosz Mitka[2] 0000-0002-1896-3126

[1] Geodetic Students Society, Faculty of Environmental Engineering and Land Surveying, University of Agriculture in Krakow
[2] Department of Agricultural Land Surveying, Cadastre and Photogrammetry, University of Agriculture in Krakow
✉ Corresponding author: hubmalyszek@gmail.com

Summary

This study provides a thorough analysis of the impact of different image file formats on the accuracy of photogrammetric studies using non-metric cameras. It specifically examines three widely used data storage formats: digital RAW negatives, lossless TIFF files, and compressed JPEG files, evaluating their effectiveness across various measurement conditions. The research involved photogrammetric measurements of two distinct test objects, providing a basis to evaluate how the choice of equipment and data format influences the quality of the resulting 3D models. The findings from this study highlight that the RAW format offers the highest quality and fidelity of detail in photogrammetric models, which is particularly crucial for professional applications where extreme accuracy is required. Conversely, the TIFF format, while balancing quality and file size, introduces minor geometric errors that might be acceptable in applications with less stringent accuracy demands. The JPEG format, although the most efficient in terms of file size reduction, shows the greatest level of distortion and the lowest level of model geometry accuracy. This is attributed to the lossy nature of JPEG compression, which significantly compromises the precision needed for high-quality photogrammetric output. Consequently, the study underscores the importance of selecting the appropriate file format based on the specific accuracy requirements of the photogrammetric task at hand.

Keywords

photogrammetry • analysis • 3D modelling • camera comparison • accuracy testing

1. Introduction

Photogrammetric surveys rely on high-quality imagery to ensure accurate geometry reproduction. The quality of these data depends on several factors [Alfio et al. 2017, Welch and Dikkers 1978], including camera optics, parameter settings (ISO, aperture, exposure time), shutter types (global, rolling), recording format, and post-processing (RAW, JPEG, TIFF). Research on non-metric analog cameras dates back to the 1970s [Welch and Dikkers 1978], forming a knowledge base that has evolved with digital technology [Gonzales and Woods 2002, Gołka and Haliński 2000]. The digital negative, RAW, converted to TIFF, is preferred for photogrammetry [Parulski and Spaulding 2003]. RAW files, processed minimally and directly from the sensor, preserve extensive information, aiding in correcting optical defects and exposure issues. However, the varied RAW formats across manufacturers complicate multi-source projects. Adobe's DGN [Digital Negative] format addresses this by standardizing RAW data, making it easier for software developers to implement. TIFF (Tagged Image File Format) [Parulski and Spaulding 2003, Sumner 2014], developed by Aldus and now owned by Adobe, is popular for its scalability and lossless compression, suitable for photogrammetric applications. However, increasing image resolution necessitates more efficient compression systems due to higher data volume. The JPEG format [Panchanathan et al. 1996], created by the Joint Photographic Experts Group, addresses this by minimizing file size. It offers lossy and lossless types of compression. Lossless compression saves about 10% of the file size with minimal pixel changes, while lossy compression significantly reduces file size but increases image distortion [Burley and Lacewell 2008]. JPEG compression involves color space conversion and down-sampling [Alfio et al. 2017]. Adobe standardizes compression from 0 to 12, with 12 indicating 93–100% fidelity to the original and 0 indicating 0–7% fidelity [Adobe Systems Inc. 2012].

2. Project objectives

The goal of this study was to compare the effect of data format and the type of compression on photogrammetric results using cameras from different markets: professional, semi-professional, and amateur [Alfio et al. 2017, Welch and Dikkers 1978].
The cameras used were a Canon 5D Mark IV with a Sigma Art 35mm lens, a DJI Mavic 2 Pro with a built-in camera, and a Samsung Galaxy S22 Ultra. The Canon is for professional photography and photogrammetry, the Mavic 2 Pro for semi-professional photogrammetric missions, and the Samsung smartphone, a consumer device not typically suited for such work [Albertz and Wiedemann 1995, Barrile et al. 2015].

The selected file formats were RAW CR2 and DNG, developed 16-bit lossless TIFF, and developed JPEG files with a compression ratio of 8 [Alfio et al. 2017, Welch and Dikkers 1978]. RAW files, chosen for their wide range of information, were processed in Agisoft Metashape version 2.0.7. Lossless 16-bit TIFF files were developed after correcting optical defects for optimal visual results [Alfio et al. 2017, Welch and Dikkers 1978, Parulski and Spaulding 2003]. JPEG images were also developed from RAW files with the same parameters as the TIFF files [Fraser 2013, Workman et al. 2015].

The first stage involved creating datasets (point clouds, 3D mesh models, textures) using all file formats in Agisoft Metashape version 2.0.7 [Kraus 1993, Linder 2013]. This included making sparse and dense point clouds, grid models, and UV textures, aligned to a unified local coordinate system [Dlesk et al. 2020, Maiwald et al. 2017]. Timing was crucial in analysing these elements. Measurements were performed on a single workstation for consistent computational power [Albertz and Wiedemann 1995, Barrile et al. 2015].

The second stage of office work involved an analysis [Gołka and Haliński 1998] that was divided into stages based on the measurement object. The first stage analyzed processing time and computing power for each file format; the second stage involved a visual analysis of reproduction factors and geometry inspection using Metashape. This concluded the analysis for objects measured under laboratory conditions. In the third stage, squared errors, residual errors, and the covariance matrix were compared for objects with photopoints measured in the field [Besl and McKay 1992]. The final stage compared noise values of the dense point clouds using Cloud Compare software [Rajendra et al. 2014].

3. Measurement of object No. 1 – controlled lighting conditions

The first set of measurements aimed to minimize the impact of external factors. The optical test room with consistent lighting was used [Boroń et al. 2007]. A rotating base was placed centrally, with the Leica Scanstation P40 laser scanner as the first measurement object due to its complex geometry and uniform surface [Stamatopoulos 2011]. Each camera was stabilized on a tripod and set to a native ISO of 100 to minimize errors and noise [Welch and Dikkers 1978]. Photos were taken from three perspectives: 40 cm above the scanner with a 30-degree downward angle; level with the scanner; and 40 cm below the scanner with a 30-degree upward angle. The base was adjusted by 10 degrees, resulting in 108 photos per camera. Each camera was set to full resolution, saving images only in RAW format (CR2 for Canon, DNG for Samsung and DJI) [Workman et al. 2015]. The measurement focused on reconstructing the object from RAW data without capturing photopoints [Hegde et al. 2012].

4. Measurement of object No. 2 – dynamic lighting conditions

The second set of measurements aimed to include the impact of external factors. The Fryderyk Chopin monument in Park Decius, Kraków, Poland, was selected as the test object. The measurement took place under favorable lighting, with an overcast sky eliminating harsh light [Mancini et al. 2016]. The complex geometry of the monument was ideal for accurate comparisons between model renderings and point clouds [Mikhail et al. 2001, Fraser 2013]. A photopoint measurement on the object's surface was performed using a TrimbleC5 total station with 1-second precision, recording 12 photopoints in 2 series (two rotations each) to minimize error [Trimble 2018]. The measurement used the local XYZ coordinate system, with no plans to transfer to a global system [Chen et al. 2014]. Photogrammetric imaging was performed using handheld cameras, with the ISO increased to 320 and an exposure time of 1/200s to prevent motion blur. Measurements were taken from two perspectives: one at about one meter high and another at two meters high, both perpendicular to the object. There were 40 photographs taken from each perspective, a total of 80 per camera. The measurements were successfully conducted, allowing the project to proceed.

5. Office work – photo development

To prepare the acquired images for further processing and to conduct analyses, it was necessary to prepare the images for additional editing. Regarding the imaging of measurement objects, these were divided into three categories: RAW, TIFF, and JPEG. The RAW format photos were left as originally captured. TIFF and JPEG format images were developed using Adobe Lightroom to extract data from shadows and eliminate overexposures. Automatic lens optical correction was also performed. The photos were neither sharpened nor denoised to preserve the accuracy of the measurements [Dlesk et al. 2020, Maiwald et al. 2017]. After development, the photos were exported in two versions: as 16-bit, uncompressed TIFF, and in JPEG format with the compression level set at 80.

6. Office work – photogrammetric works in Agisoft Metashape

To prepare the photogrammetric products, data processing was conducted in Agisoft Metashape software. The processing involved initially aligning the images, and for object number 2, fitting the preliminarily aligned photos into the local reference system. This was followed by generating a dense point cloud based on depth maps obtained from the captured images [Remondino et al. 2011]. The next step was to create a mesh model based on the aforementioned depth maps and to overlay the model with texture in the form of two 8k resolution UV maps [Westoby et al. 2012]. It was planned to produce 9 scanner models and 9 monument models, all according to the same batch processing scheme [Szeliski 2010]. The scheme included the following steps with the given parameters:

1. *Align Photos*: medium accuracy, no generic preselection, key point limit of 20000, tie point limit of 6000, no masking, exclusion of stationary tie points, no guided image matching, and with fixed camera model fitting. Additionally, for the monument model, fitting the model into the local system and aligning the results was required.
2. *Build Dense Cloud*: medium quality, aggressive depth filtering, with calculations of point colors and point confidence.
3. *Build Mesh*: using depth maps as source data, arbitrary surface type, medium face count, aggressive depth filtering, interpolation on, without calculating vertex colors.
4. *Build Texture*: generic mapping mode, mosaic blending mode, 2x8192 textures, with hole filling and ghosting filter. The assumptions were not to clean the point cloud in order to check the number of unwanted elements generated [Barrile et al. 2015]. A report was generated for each of the 18 created models. For the monument

processing, dense point clouds were exported in .laz format. Orthogonal projections of the model fronts were exported in three versions: textured, reproduction fidelity coefficient, and full mesh. These images were used for visual analysis to assess rendering quality [Panchanathan et al. 1996].

7. Office work – analysis

Optical analysis facilitated the determination of possible fidelity of reproduction, chromatic aberration, distortion, and depth of field, enabling the most accurate depiction of the photogrammetric products created [Fraser 2013]. After completing the postprocessing tasks in Agisoft Metashape, data analysis commenced [Scianna and La Guardia 2017, Tinkham and Swayze 2021]. The analysis was divided into two parts.

7.1. Visual analysis in Agisoft Metashape

This analysis covered all the created models (9 scanner models and 9 monument models). Comparisons were made based on texturing quality, reproduction fidelity, and overall topology [Scianna and La Guardia 2017]. Initially, the Canon camera's photogrammetric products were evaluated (Fig. 1), showing models based on RAW, 16-bit TIFF, and 8-bit JPEG formats [Kingsland 2020].

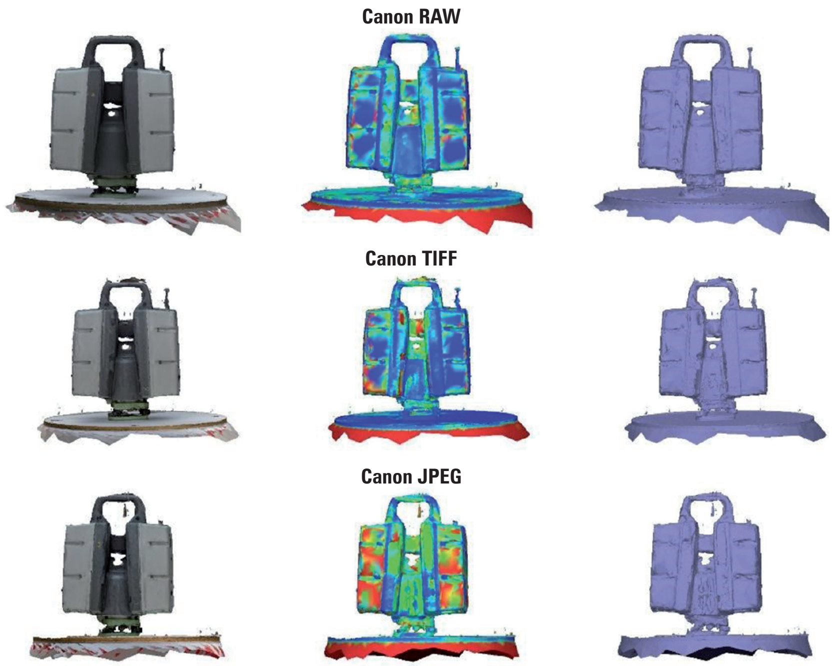

Source: Authors' own study

Fig. 1. Canon visual analysis

Starting from the left, we see the texturing of the model, the fidelity of reproduction coefficient (blue for correct values, red for reproduction errors), and the model without texture [Howland et al. 2022]. For RAW files, the model geometry is accurate with fine details, and the fidelity of reproduction is high – few shifts toward red, despite working with reflective surfaces and complex geometry. The texture is correctly executed without artifacts or illegible spaces [Panchanathan et al. 1996]. The situation changes with the model based on TIFF. Despite extracting all possible details and removing overexposures, the resultant product significantly deviates from the RAW model. Geometric distortions become visible, reducing the fidelity of reproduction coefficient, and the texture loses details and sharpness [Fraser 2013]. The model based on JPEG performs even worse—significant changes in geometry, over 80% error in the reproduction coefficient, and the worst texture quality of all [Chang and Tan 2004].

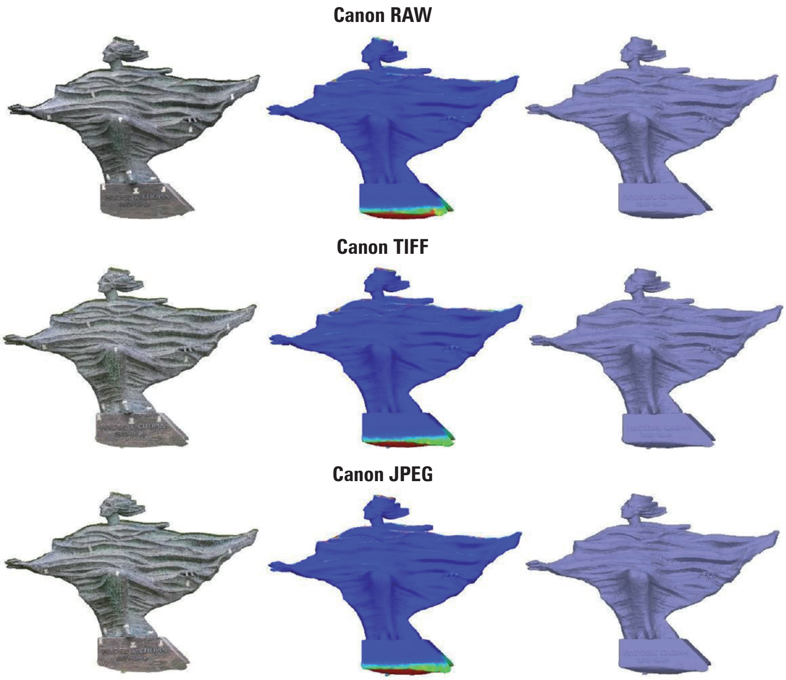

Source: Authors' own study

Fig. 2. Canon visual analysis

The monument model was then analyzed (Fig. 2). Despite its complex geometry, it was easier to digitally reconstruct due to its rough, non-reflective surface. We can see the advantage of RAW files, although it is not as significant as in case of the scanner, due to the aforementioned ease of digital reconstruction of the model. The model based on RAW exhibits exemplary accuracy and detail, with the fidelity of reproduction coefficient showing no significant deviations, and the texture is sharp and precise [Orych et al. 2014]. The model created using TIFF also presents high quality, with minimal errors in the fidelity of reproduction coefficient and geometry, and the quality of texture is also good [Orych et al. 2014]. Similarly, the evaluation of the model based on JPEG shows slightly lower quality than TIFF, in terms of both geometry and fidelity of reproduction. However, the texture quality and clarity remains good [Daakir et al. 2019].

Next, the products created using the DJI Mavic 2 Pro were reviewed, starting with the scanner models (Fig. 3). The model based on RAW shows significantly lower quality than the model based on the same file type created by Canon. There are visible errors in geometry, and a substantial amount of the fidelity of reproduction coefficient error is present. Nonetheless, the texturing is performed at an acceptable level [Giuliano 2014]. The situation worsens with TIFF - holes begin to appear in the object, and the topology of the object ceases to be acceptable [Fraser 2013]. The fidelity of reproduction coefficient noticeably shifts towards red [Reina Ortiz et al. 2019]. The texture is incorrectly executed [Kabadayi and Erdoğan 2022]. A model based on JPEG was not possible to obtain, as the photos were unable to correctly align [Hegde et al. 2012].

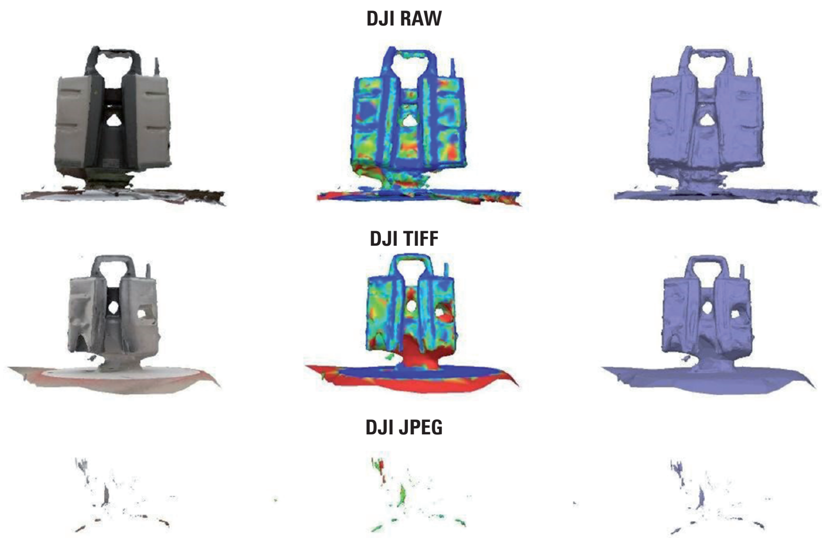

Source: Authors' own study

Fig. 3. DJI visual analysis

The next step in the analysis was the evaluation of the monument models (Fig. 4). Here, the results further confirm the quality of models made from RAW. There are no significant errors in topology, minimal errors in fidelity of reproduction are visible, and the texture is sharp and clear [Clevy 2013]. For the model made using TIFF, there is a significant regression compared to RAW – some elements of the monument could not be reconstructed, and those that were reconstructed show errors in topology, which in turn deteriorated the fidelity of reproduction coefficient [Albertz and Wiedemann 1995]. The texture loses sharpness and accuracy [Kiefner and Hahn 2000]. An even greater error characterization is observed in the model made from JPEG – in addition to missing parts of the monument, there are added distortions. The fidelity of reproduction coefficient is lower than in the TIFF case, and the texture also visibly loses quality.

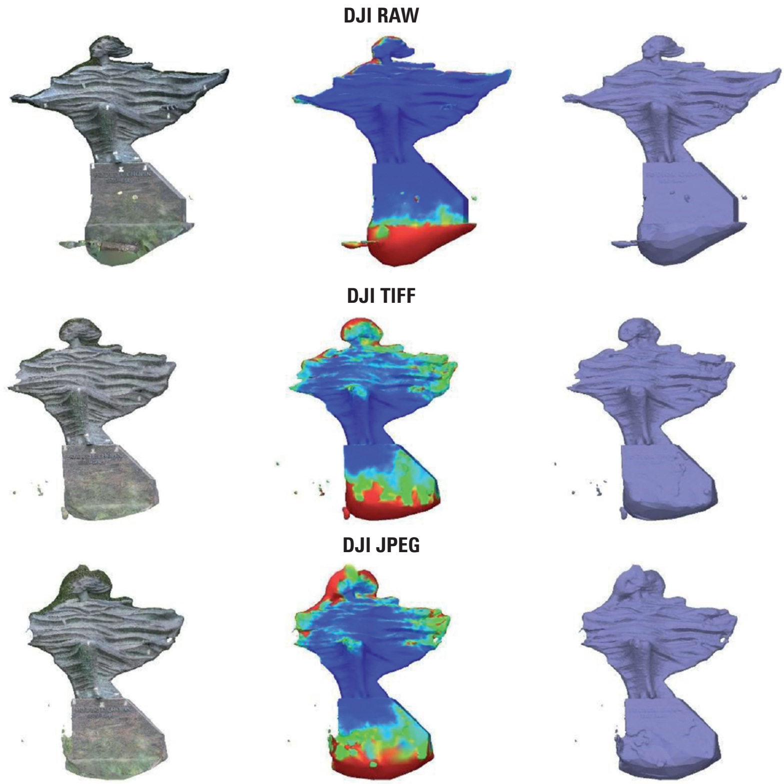

Source: Authors' own study

Fig. 4. DJI visual analysis

The final component of the visual analysis involved evaluating the products made using the Samsung camera, starting with a comparison of the scanner models (Fig. 5). Even in the RAW file, significant geometric errors and holes in the model are visible, resulting in a low fidelity of reproduction coefficient and a poorly matched, low-quality texture. The model based on TIFF shows a complete lack of utility – very large errors in the model's topology, gaps, and a failure to reconstruct details [Parulski and Spaulding 2003]. The fidelity of reproduction coefficient is noticeably shifted towards red, and the texture is blurry and poorly matched. The model created using JPEG lacks any details, the topology is incorrect, and the fidelity of reproduction coefficient exhibits very large errors. The texture is incorrect, blurry, and poorly fitted.

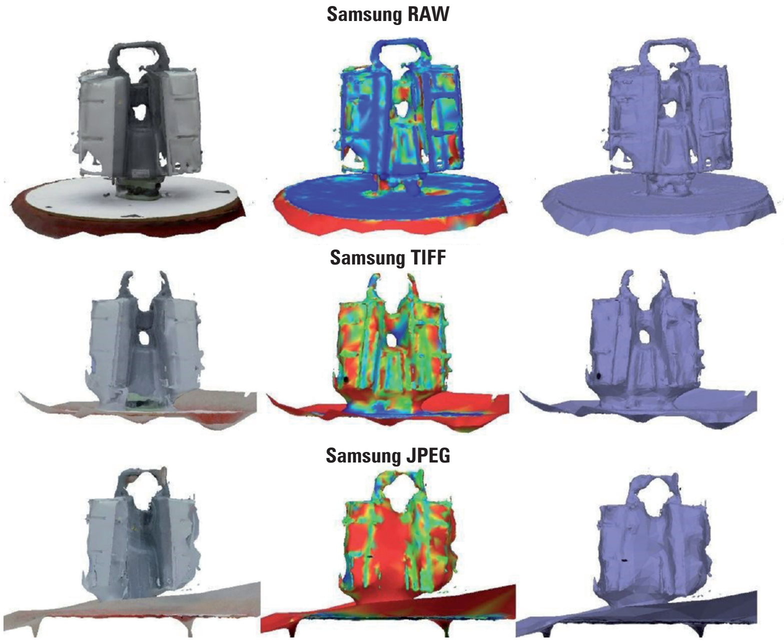

Source: Authors' own study

Fig. 5. Samsung visual analysis

The models of the monument (Fig. 6) are rather suprising. The object created from RAW does not exhibit major errors in geometry or fidelity of reproduction, and the texture is sharp and correctly matched. However, the model made from TIFF has significant errors in geometry, significantly increasing the fidelity of reproduction coefficient. Consequently, the texture in this case has holes and blurriness. On the other hand, there are no significant differences between the model based on JPEG and the model based on RAW. There are sporadic topology errors, but they do not affect the fidelity of reproduction coefficient in any considerable way. The texture is sharp and contains a high level of detail.

7.2. Point cloud analysis

The final analysis involved a comparison of the dense point clouds of the monument models. This was possible by embedding all clouds in the local coordinate system using measured photopoints. Four comparisons were made: vertical cross-section of the cloud divided by cameras (Fig. 7) and vertical cross-section divided by file types (Fig. 8).

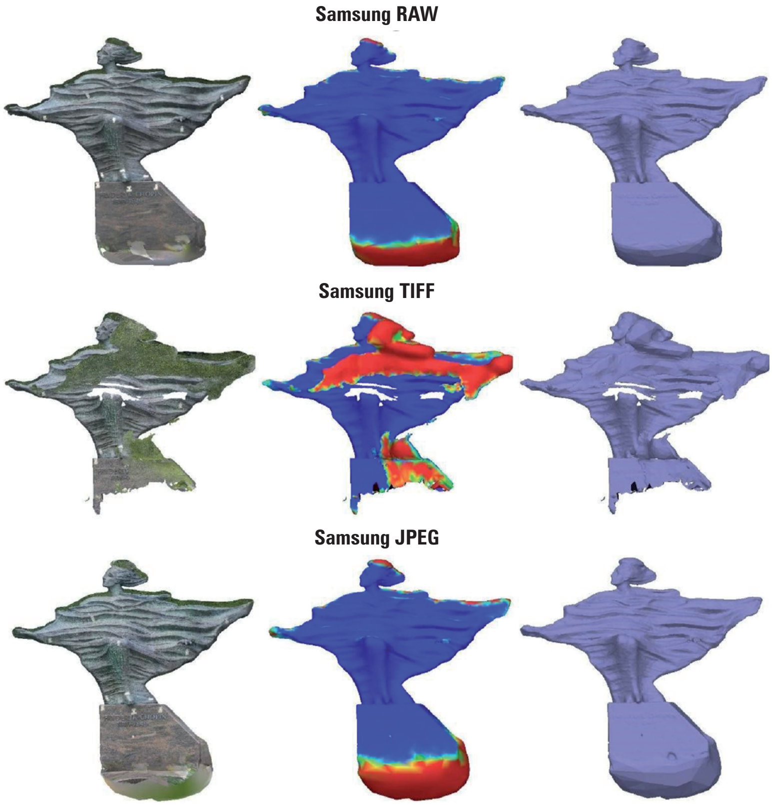

Source: Authors' own study

Fig. 6. Samsung visual analysis

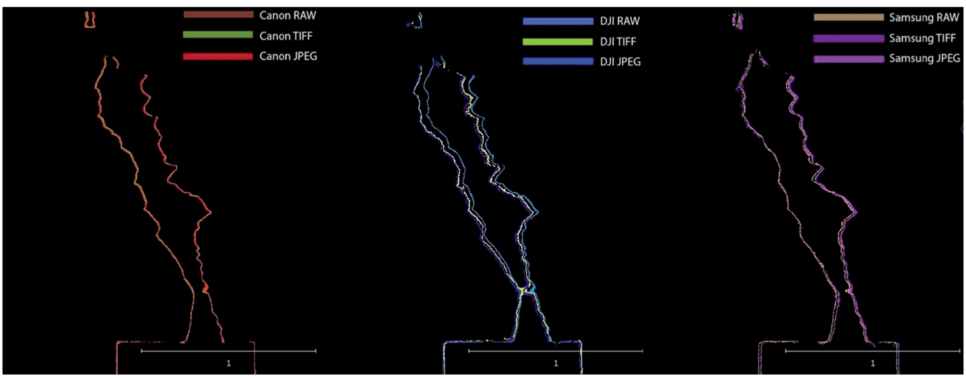

Source: Authors' own study

Fig. 7. Vertical cloud cross-section comparison by camera

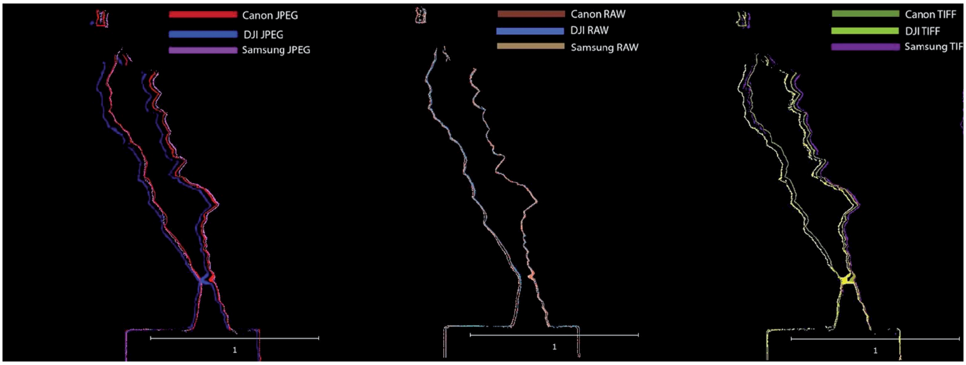

Source: Authors' own study

Fig. 8. Vertical cloud cross-section comparison by photo type

The vertical cross-section analysis showed uniformity and repeatability of measurements with the Canon camera, with Samsung were second best, and the DJI performed the worst. This is surprising given DJI's higher resolution sensor. Notably, clouds made from RAW files demonstrated great uniformity regardless of the camera model. RAW files showed the highest repeatability, while TIFF and JPEG performed worse in this regard.

8. Discussion

The results obtained from the measurements of two test objects and the creation of 18 models with identical parameterization of the work, clearly demonstrate the impact of sensor resolution and photo format on subsequent processing [Gonzalez-Jorge et al. 2015]. While the resolution issue seems obvious, the photo format aspect revealed a significant advantage of RAW files over TIFF and JPEG files. Regardless of the camera used, each test object was most accurately digitally reconstructed using RAW files, preserving the most information about the object's geometry, presenting high fidelity of reproduction, and enabling precise texturing of the model later [Moussa et al. 2013]. Additionally, a comparison of the point clouds of the models after fitting to the local coordinate system demonstrated the greatest accuracy in both transverse and vertical cross-sections using RAW format files. TIFF, a lossless format, ranked second with results noticeably worse than RAW. JPEG files with lossy compression were the least useful for precise photogrammetric measurements, cutting off a significant portion of information. However, the results suggest that the JPEG format is best suited for photogrammetric tasks that are repeated regularly and do not require high precision, such as monitoring construction progress with 3D models, documenting landscape changes, or creating quick overviews of large areas. Its smaller file size and faster processing make it ideal for routine applications where efficiency is prioritized over extreme detail. On the other hand, TIFF and RAW formats excel in tasks requiring millimeter-level accuracy, such as digital archiving of historical monuments or precise engineering measurements, where preserving geometric fidelity and enabling fine texturing are essential.

9. Summary

The comprehensive studies assessed the models created with different quality cameras using three different photo formats – RAW digital negatives, lossless 16-bit TIFF files, and 8-bit JPEGs with lossy compression. The images were developed in the three formats, and 9 models were prepared for each object, totaling 18 photogrammetric products. These objects were subjected to a multi-level analysis to evaluate the impact of the photo format on the final quality. The results highlighted clear differences in model quality depending on the photo format. The RAW format, despite requiring more processing time, provided the best detail fidelity and the least geometric distortions. These models also featured the highest quality textures and the smallest positioning errors. TIFF provided good results but had some limitations in detail reproduction and greater geometric errors than RAW. JPEG was the least effective, introducing the most distortions and artifacts, significantly lowering the final product quality. The study also demonstrated the utility of various cameras for photogrammetric tasks, including a mobile phone camera. Although initially unconventional, the smartphone camera performed well. The studies showed that the choice of photo format is critical to the quality of photogrammetric models. For the highest quality and accuracy, the RAW format is preferred despite higher hardware and time requirements. The TIFF format offers a compromise between quality and efficiency, while JPEG is best for projects prioritizing processing speed and data size over precision [Luhmann et al. 2021, Fryer et al. 2007, Remondino and El-Hakim 2006].

References

Adobe Systems Inc. Digital Negative Specifications. 2012.

Albertz J., Wiedemann A. 1995. From Analogue to Digital Close-Range Photogrammetry. Proceedings of the First Turkish-German Joint Geodetic Days. Istanbul, Turkey, 245–253.

Alfio V.S., Costantino D., Pepe M. 2020. Influence of image TIFF format and JPEG compression level in the accuracy of the 3D model and quality of the orthophoto in UAV. Journal of Imaging, 11, 6(5), 30.

Baqersad J., Poozesh P., Niezrecki C., Avitabile P. 2017. Photogrammetry and optical methods in structural dynamics – A review. Mechanical Systems and Signal Processing, 1, 86, 17–34.

Barrile V., Bilotta G., Lamari D., Meduri G.M. 2015. Comparison between techniques for generating 3D models of cultural heritage. Recent Advances in Mechanics, Mechatronics, Civil, Chemical and Industrial Engineering, Mathematics, and Computer Science and Engineering Series, 49, 140–145.

Besl P., McKay N. 1992. A method for registration of 3-d shapes. IEEE Transactions on Pattern Analysis and Machine Intelligence, 14(2), 239–256.

Boroń A., Rzonca A., Wróbel A. 2007. The digital photogrammetry and laser scanning methods used for heritage documentation. Roczniki Geomatyki, 5(8), 129–140 (in Polish).

Burley B., Lacewell D.P. 2008. Ptex: Per-face texture mapping for production rendering. Eurographics Association, 1155–1164.
Chang E., Cheung S., Pan D. 1999. Color filter array recovery using a threshold-based variable number of gradients. Proceedings of SPIE, 3650, 36.
Chang N.L., Tan N.Y.P. 2004. Effective use of spatial and spectral correlations for color filter array demosaicking. IEEE Transactions on Consumer Electronics, 50(1), 355–365.
Clevy L. 2013. Inside the Canon RAW format version 2.
Daakir M., Zhou Y., Deseilligny M.P., Thom C., Martin O., Rupnik E. 2019. Improvement of photogrammetric accuracy by modeling and correcting the thermal effect on camera calibration. ISPRS Journal of Photogrammetry and Remote Sensing, 148,142–155.
Dlesk A., Uueni A., Vach K., Pärtna J. 2020. From Analogue to Digital Photogrammetry: Documentation of Padise Abbey in two different time stages. Applied Sciences, 10(23), 8330.
Fraser C.S. 2013. Automatic camera calibration in close range photogrammetry. Photogrammetric Engineering and Remote Sensing, 79(4), 381–388.
Giuliano M.G. 2014. Cultural Heritage: An example of graphical documentation with automated photogrammetric systems. International Archives of the Photogrammetry, Remote Sensing and Spatial Information Sciences, XL-5, 251–255.
Gołka J., Haliński J. 1998. The use of digital photogrammetry in architectural studies on the example of the front elevation of the Town Hall in Zamość. Archiwum Fotogrametrii, Kartografii i Teledetekcji, 8 (in Polish).
Gołka J., Haliński J. 2000. Digital photogrammetry in architecture – new possibilities for stocktaking and archiving objects. Archiwum Fotogrametrii, Kartografii i Teledetekcji, 10 (in Polish).
Gonzales R.C., Woods R.E. 2002. Digital image processing. 2nd ed. Prentice Hall, Upper Saddle River, NJ, p. 797.
Hegde G.P., Hegde N., Muralikrishna I. 2012. Measurement of quality preservation of pansharpened image. International Journal of Engineering Research and Development, 2, 12–17.
Hermanowski A. 1978. Mean observation errors in horizontal grids aligned with tie-in conditions. Instytut Geodezji i Kartografii (in Polish).
Howland M.D., Tamberino A., Liritzis I., Levy T.E. 2022. Digital deforestation: Comparing automated approaches to the production of digital terrain models (DTMs) in Agisoft Metashape. Quaternary, 14, 5(1), 5.
Ippoliti E., Meschini A., Sicuranza F. 2015. Structure from motion systems for architectural heritage. A survey of the internal loggia courtyard of Palazzo del Capitani Ascoli Piceno, Italy. International Archives of the Photogrammetry, Remote Sensing and Spatial Information Sciences, XL-5/W4, 53–60.
Kabadayi A., Erdoğan A. 2022. Application of terrestrial photogrammetry method in cultural heritage studies: A case study of Seyfeddin Karasungur. Mersin Photogrammetry Journal, 4(2), 62–67.
Kiefner M., Hahn M. 2000. Image compression versus matching accuracy. International Archives of the Photogrammetry, Remote Sensing, 33, 316–323.
Kingsland K. 2020. Comparative analysis of digital photogrammetry software for cultural heritage. Digital Applications in Archaeology and Cultural Heritage, 18, e00157.
Kraus K. 1993. Photogrammetry. Dümmler, Bonn.
Linder W. 2013. Digital photogrammetry: theory and applications. Springer Science & Business Media.
Maiwald F., Vietze T., Schneider D., Henze F., Münster S., Niebling F. 2017. Photogrammetric analysis of historical image repositories for virtual reconstruction in the field of digital hu-

manities. International Archives of the Photogrammetry, Remote Sensing and Spatial Information Sciences, XLII-2/W3, 447–452.

Orych A., Walczykowski P., Jenerowicz A., Zdunek Z. 2014. Impact of the cameras radiometric resolution on the accuracy of determining spectral reflectance coefficients. International Archives of the Photogrammetry, Remote Sensing and Spatial Information Sciences, XL-1, 347–349.

Panchanathan S., Gamaz N., Jain A.K. 1996. JPEG based scalable image compression. Computer Communications, 1, 19(12), 1001–1013.

Parulski K., Spaulding K. 2003. Color image processing for digital cameras. In: Digital Color Imaging Handbook, 728–757.

Rajendra Y.D., Mehrotra S.C., Kale K.V., Manza R.R., Dhumal R.K., Nagne A.D. 2014. Evaluation of partially overlapping 3D point cloud's registration by using ICP variant and Cloud-Compare. International Archives of the Photogrammetry, Remote Sensing and Spatial Information Sciences, XL, 8, 891–897.

Reina Ortiz M., Yang C., Weigert A., Dhanda A., Min A., Gyi M., Su S., Fai S., Santana Quintero M. 2019. Integrating heterogeneous datasets in HBIM of decorated surfaces. International Archives of the Photogrammetry, Remote Sensing and Spatial Information Sciences, XLII-2/W,15, 981–988.

Scianna A., La Guardia M. 2017. Main features of a 3D GIS for a monumental complex with historical-cultural relevance. International Archives of the Photogrammetry, Remote Sensing and Spatial Information Sciences, 42, 519–526.

Smith M.J., Priestnall G., Asal F. 2000. Combining LIDAR and photogrammetry for urban and rural landscape studies. International Archives of the Photogrammetry, Remote Sensing, 33(B3), 44–50.

Stamatopoulos C. 2011. Orientation and calibration of long focal length cameras in digital close-range photogrammetry. Ph.D. thesis. The University of Melbourne.

Sumner R. 2014. Processing raw images in matlab. Department of Electrical Engineering, University of California Santa Cruz, 2.

Tinkham W.T., Swayze N.C. 2021. Influence of Agisoft Metashape parameters on UAS structure from motion individual tree detection from canopy height models. Forests, 22, 12(2), 250.

Welch R., Dikkers K. 1978. Educational and research aspects of non-metric, close range analogue photogrammetry. Photogrammetric Record, 1, 9(52), 537–547.

Workman S., Greenwell C., Zhai M., Baltenberger R., Jacobs N. 2015. Deepfocal: A method for direct focal length estimation. IEEE International Conference on Image Processing (ICIP), 1369–1373.